

Low Complexity Cooperative Relay NOMA Systems: Analytical Evaluation in κ - μ Fading with Imperfect SIC

Said Awad and Mohammed Abdel-Hafez *

Department of Electrical and Communication Engineering, United Arab Emirates University, United Arab Emirates
Email: 201990104@uaeu.ac.ae (S.A.); mhafez@uaeu.ac.ae (M.A-H.)

*Corresponding author

Abstract—This research investigates the performance of a low complexity Cooperative Relay System (CRS) integrated with Non-Orthogonal Multiple Access (NOMA) over κ - μ fading channels. The system model consists of two users receiving information from a source through direct and relayed links. Key performance metrics, including outage probability and achievable rate, are analyzed in depth. To achieve this, we derive the Probability Density Functions (PDFs) and Cumulative Distribution Functions (CDFs) of the received instantaneous Signal-to-Noise Ratios (SNRs) for both direct and relayed transmissions. These distributions then formulate users' outage probability and average achievable rate expressions. Additionally, we derive outage probability expressions under the assumption of CRS-NOMA with imperfect Successive Interference Cancellation (SIC). The study further explores the impact of relay-to-user distance on system performance and the influence of κ - μ fading channel parameters. A major challenge in conventional CRS-NOMA systems is the reliance on complex power allocation techniques, where symbols must be transmitted with carefully controlled power levels. This adds significant computational complexity and increases system design overhead. To address this, we propose an alternative CRS-NOMA scheme that eliminates the need for power allocation by enabling each symbol to be transmitted at maximum power. This simplification reduces processing complexity and enhances system efficiency, making the proposed model more practical for real-world applications. Monte Carlo simulations are conducted to validate the analytical findings.

Keywords—cooperative NOMA, outage probability, achievable rate, imperfect SIC, half-duplex.

I. INTRODUCTION

The growing need for mobile internet and the Internet of Things (IoT) presents demanding requirements for 5G wireless communications, including high spectral efficiency and extensive connectivity [1, 2]. The increasing demands have necessitated the exploration of new developments in multiplexing techniques. This is because the current Orthogonal Multiple Access (OMA)

techniques employed by wireless communication systems to allocate resources to various users and applications are not anticipated to meet these demands [3]. Non-Orthogonal Multiple Access (NOMA), a crucial technology for Fifth-Generation (5G) wireless networks and beyond, facilitates meeting diverse requirements such as low latency, high reliability, extensive connectivity, fairness enhancement, and increased throughput [4]. Contrary to OMA, NOMA's fundamental concept involves leveraging power domain diversity to cater to multiple users concurrently across identical time and frequency resources, employing Successive Interference Cancellation (SIC) receivers [5]. Awad and Hafez [6] investigated the achievable rate of a downlink NOMA system over κ - μ fading channels, Awad and Hafez [7] explored the outage performance of a downlink NOMA system with imperfect SIC over κ - μ fading channels.

Cooperative relaying effectively mitigates channel impairments such as fading, path loss, and shadowing, thereby extending communication coverage [8]. A basic cooperative relaying network comprises three nodes: the source, the relay, and the destination. Messages are transmitted from the source to the destination with the aid of the relay, which necessitates additional orthogonal bandwidth resource blocks. For instance, two-time slots are typically required for transmission completion in a time division multiple access system. During the first slot, the source broadcasts the signal to both the relay and the destination, and during the second slot, the relay forwards the information received from the source to the destination. Two widely recognized relay protocols are the Amplify-and-Forward (AF) and Decode-and-Forward (DF) protocols. The AF relay relays a scaled version of its observation to the destination, while the DF relay first attempts to decode the received signal and retransmits the decoded information to the destination. Both relay protocols have been extensively studied in the literature within the context of conventional Orthogonal Multiple Access (OMA) systems [9].

NOMA offers characteristics that present prospects for enhanced performance and more efficient spectral utilization within downlink cooperative networks [10]. Recently, there has been a notable increase in research

interest worldwide regarding integrating NOMA into cooperative networks [11, 12]. Particularly, Lv *et al.* [11] studied the outage performance of a cognitive radio system assisted with NOMA over Rayleigh block-fading. Singh and Bansal [12] proposed a downlink NOMA-based Cooperative Relay System (CRS) and investigated the outage probability of the system over Rayleigh fading channels. Further, authors have investigated the performance of a CRS-NOMA in Ref. [13], where a single antenna source communicates with two single-antenna users via a direct link and through a single-antenna DF relay over Nakagami- m fading channels. The Symbol Error Probability (SEP) of a cooperative downlink NOMA system over Rayleigh fading has been investigated in Ref. [14], where a Base Station (BS) communicates with near and far users via two-half duplex DF relays. Wu *et al.* [15] presented an achievable rate analysis of a CRS-based NOMA with imperfect Successive Interference Cancellation (SIC) over κ - μ fading channels where a single-antenna source communicates with a single-antenna user through a single-antenna half-duplex DF relay.

Recently, the Physical Layer Security (PLS) of a Cognitive Radio (CR)-inspired downlink NOMA (CR-NOMA) network has been investigated in Ref. [16], where a single-antenna source communicates with two users via a DF relay while an eavesdropper is also present in the network. Moreover, Yue *et al.* [17] investigated the performance of the CRS-NOMA network over Nakagami- m fading channels where the source transmits its information to two users via an AF relay. Kurup *et al.* [18] presented the outage performance analysis of a two-user cooperative downlink NOMA network over log-normal fading channels where the base station communicates with two users: a strong (near) user and a weak (far) user. With the direct link between the BS and weak user assumed to be very weak, the BS is expected to employ a strong user as a Half-Duplex (HD) relay to deliver the transmitted message to the weak user. Kumar and Flanagan [19] present the performance analysis of a CRS-NOMA network, which consists of a BS, a DF-relay, and a user over α - μ fading channels. Further, Jiao *et al.* [20] investigated the average achievable rate of a similar system as presented in Ref. [19] over Rician channels. Li *et al.* [21] investigated the performance of a CRS-NOMA network with two source-user pairs where two sources and two users share a single DF relay over Rayleigh fading channels. It can be noted from Refs. [11–22] that in the CRS-NOMA systems presented in these research works, in the first time slot, the source transmits the superposition of two different symbols to the relay (or relays) and user (or users) and in the second time slot, only the relay transmits the decoded symbols to the user (or users). The source does not transmit any symbol in the second time slot. Nonetheless, the majority of current schemes overlook the transmission of source symbols during the second time slot, limiting their ability to leverage the full potential of the NOMA principle for enhanced performance. Moreover, these schemes

necessitate high-complexity power allocation to achieve optimal data rates.

To address these limitations, a CRS-NOMA scheme was proposed in Ref. [23] to improve the system's performance. This scheme comprises a single-antenna source, a half-duplex DF relay, and a single-antenna destination. In the proposed CRSNOMA scheme, the source transmits one symbol to both the relay and the destination during the first time slot. Then, in the second time slot, the source transmits another symbol directly to the destination with the same power, while the relay transmits the decoded symbol to the destination. Finally, the destination decodes the symbols by exploiting the SIC detection scheme.

Furthermore, the performance of this system was investigated in Ref. [23] over Rayleigh fading. Further, the achievable rate of the CRS-NOMA system, proposed in Ref. [23], over Rician fading channels has been analyzed in Ref. [24]. Moreover, Khatalin and Hadeel [25] investigated the performance of the same system as proposed in Ref. [23] over κ - μ fading channels in terms of outage probability and achievable rate.

Our literature analysis shows that the performance analysis of the CRS-NOMA scheme proposed in Ref. [14] is limited. The works presented in Refs. [23–26] have investigated the performance of the proposed system in Ref. [14] over various fading channels, such as Rayleigh, Rician, Nakagami- m , and κ - μ fading channels. However, they have considered the presence of only one user. To the best of the author's knowledge, none of these works have investigated the performance of the CRS-NOMA scheme proposed in Ref. [26] for more than one user. We also notice that the studies on the performance analysis of such systems over generalized fading channels, such as κ - μ and α - μ , are limited. The κ - μ distribution is a comprehensive fading distribution encompassing the well-known fading distributions, specifically the Rice and Nakagami- m distributions. It is essential to observe that the Rice and Nakagami distributions encompass the Rayleigh distribution. Furthermore, the Nakagami- m distribution encompasses the One-Sided Gaussian distribution. Thus, it is also possible to derive these distributions from the κ - μ distribution.

Motivated by the features offered by the CRS-NOMA scheme proposed in Ref. [25] and the research gaps discussed above, we study the performance of a two-user CRS-NOMA network (as shown in Fig. 1) over κ - μ fading channels in terms of the outage probability and achievable rate. In our considered system, a single-antenna source S communicates with two single-antenna users, D_1 and D_2 , directly and through a half-duplex decode-and-forward DF relay. The signal transmission scheme in our considered CRS-NOMA network is similar to the CRS-NOMA scheme proposed in Ref. [25]. In this paper, we first derive the Cumulative Distribution Functions (CDFs) and the Probability Density Functions (PDFs) of the instantaneous end-to-end SNRs at the users and the relay node for symbols x_1 and x_2 . By utilizing these derived CDFs and PDFs, we further derive the Outage Probability (OP) expressions and the users' achievable rate for the symbols

x_1 and x_2 . We investigate the impact of various parameters, such as average received SNR and fading parameters, on the system's performance. Further, we validate our analytical findings with the Monte-Carlo simulations. By removing intricate power-control mechanisms, we reduce real-time complexity and simplify the system design (compared to conventional CRS-NOMA). This approach also improves practical feasibility because each transmitter uses full power without adaptive allocation.

Section II describes the system & channel models, clarifying κ , μ , and introducing the key assumptions (perfect vs. imperfect SIC). Section III gives outage derivations with intermediate steps. Section IV addresses achievable rates. Section V discusses extensive numerical results with the Monte Carlo setup. Finally, Section VI concludes with design insights and future directions.

II. SYSTEM AND CHANNEL MODELS

In this paper, we study the performance of a downlink CRS-NOMA scenario shown in Fig. 1, where a single antenna source S wants to communicate with two single-

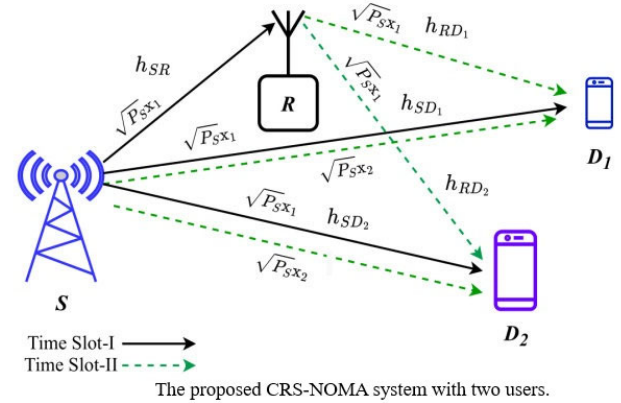
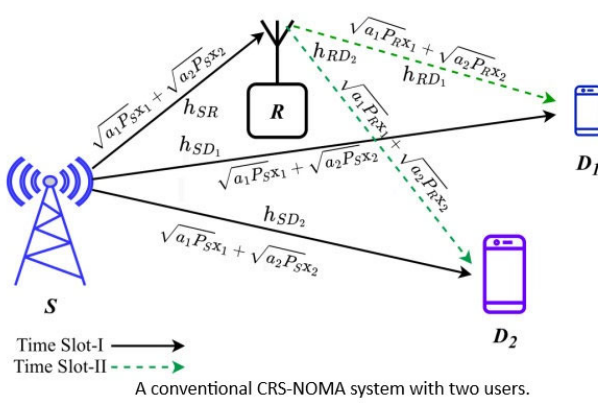


Fig. 1. CRS-NOMA systems.

In practice, residual interference remains after subtracting the strong user's signal. We model this via a factor $0 < \beta < 1$ in Eq. (8), which quantifies the fraction of uncanceled interference. When $\beta = 0$, the cancellation is perfect.

We propose a different scenario illustrated in Fig. 1(b), where each symbol can be transmitted with the maximum power to avoid the complex power allocation technique. In our considered system, the source S transmits symbol x_1 to the nodes R , D_1 , and D_2 with transmit power P_S in the first time slot, and symbol x_2 , with power P_S , is transmitted from S to D_1 and D_2 in the second time slot. Also, R transmits x_1 to the users D_1 and D_2 in the second slot with power P_S .

A. Signal Processing

In the first time slot, S transmits the symbol x_1 with power P_S . Therefore, the signal received at the nodes R and D_i for $i \in \{1, 2\}$, respectively, can be given as

$$y_{R,I} = h_{SR}\sqrt{P_S}x_1 + n_R, \quad (1)$$

$$y_{D_i,I} = h_{SD_i}\sqrt{P_S}x_1 + n_{D_i}, \quad (2)$$

antenna users, D_1 and D_2 , via a half-duplex Decode-and-Forward (DF) relay R . In the considered communication system, the source S can communicate with D_1 and D_2 through direct link and via R , where D_1 is located far from S , whereas D_2 is placed somewhere close to S . The perfect Channel State Information (CSI) of the receivers D_1 and D_2 are considered to be known to the source S . The channel coefficient between the nodes follows the κ - μ fading. The channel coefficients between the nodes $S-R$, $R-D_1$, $S-D_1$, and $S-D_2$ are denoted by h_{SR} , h_{RD_i} , h_{SD_1} , and h_{SD_2} with average powers Ψ_{SR} , Ψ_{RD_i} , Ψ_{SD_1} , and Ψ_{SD_2} , respectively.

In a traditional CRS-NOMA scenario [22, 23], shown in Fig. 1(a), the source transmits the superposition signal consisting of both symbols in the first time slot, and the receiver receives only the symbols transmitted from R in the second time slot. This scheme requires a complex power allocation technique to transmit the symbols. To avoid this complexity, the CRS-NOMA scheme presented in Ref. [26] can be exploited to improve performance without applying the power allocation methodology.

where n_R and n_D are noises at the nodes R and D_i , respectively. These noises are modeled as additive white Gaussian noise (AWGN) with zero mean and variance N_0 .

Here, Eqs. (1–2) represent the first-slot signals. We later split the SNR derivations to show how outage expressions follow from Eqs. (4–7).

In the second time slot, S transmits the symbol x_2 to receivers D_1 and D_2 with power P_S . Meanwhile, R transmits the symbol x_1 to D_1 and D_2 . Therefore, the received signals at the nodes D_i , for $i \in \{1, 2\}$, can be expressed as:

$$y_{D_i,II} = h_{RD_i}\sqrt{P_S}x_1 + h_{SD_i}\sqrt{P_S}x_2 + n_{D_i}. \quad (3)$$

B. Instantaneous End-to-End SNR

The received instantaneous signal-to-noise ratio (SNR) for x_1 in the first time slot at R and $D_i \in \{D_1, D_2\}$, respectively, can be expressed as:

$$\gamma_{SR,x_1} = \rho |h_{SR}|^2, \quad (4)$$

$$\gamma_{SD_i,x_1} = \rho |h_{SD_i}|^2 = \gamma_{SD_i}, \quad (5)$$

where $\rho = \frac{P_S}{N_0}$ denotes the transmit SNR.

As per the NOMA protocol, users $D \in \{D_1, D_2\}$ first decode x_1 by assuming x_2 as noise; further, x_1 will be removed by applying perfect SIC to decode x_2 . Therefore, in the second time slot, the received instantaneous SNRs can be obtained for symbols x_1 and x_2 at D_i , respectively, as:

$$\gamma_{SRD_i, x_1} = \frac{\rho |h_{RD_i}|^2}{\rho |h_{SD_i}|^2 + 1} = \frac{\gamma_{RD_i}}{\gamma_{SD_i} + 1}, \quad (6)$$

$$\gamma_{SD_i, x_2} = \rho |h_{SD_i}|^2 = \gamma_{SD_i}. \quad (7)$$

In practical scenarios, with imperfect SIC, it is difficult to remove x_1 due to the presence of residual interference completely. Therefore, the received SNR for symbol x_2 at the receivers with imperfect SIC can be expressed as:

$$\gamma_{SD_i, x_2}^{\mathcal{P}} = \frac{\rho |h_{SD_i}|^2}{\beta \rho |h_{RD_i}|^2 + 1} \quad (8)$$

where β denotes the level of residual interference with $0 < \beta < 1$.

C. Statistics of end-to-end Instantaneous SNRs

The Probability Density Function (PDF) and Cumulative Distribution Function (CDF) of the instantaneous SNR γ over κ - μ fading channel are given, respectively, as Ref. [27]:

$$f_\gamma(x) = \frac{\mu}{\kappa^{\frac{\mu-1}{2}} e^{\mu\kappa}} \left(\frac{1+\kappa}{\Psi} \right)^{\frac{\mu+1}{2}} x^{\frac{\mu-1}{2}} e^{-\frac{\mu(1+\kappa)}{\Psi}x} \times I_{\mu-1} \left(2\mu \sqrt{\frac{\kappa(1+\kappa)x}{\Psi}} \right) \quad (9)$$

and

$$F_\gamma(x) = 1 - \mathcal{Q}_\mu \left(\sqrt{2\kappa\mu}, \sqrt{\frac{2\mu(\kappa+1)x}{\Psi}} \right) \quad (10)$$

where κ denotes the ratio of the total power of the dominant components to the power of the scattered waves, parameter μ represents the number of multipath clusters, and Ψ is the average received SNR. $I_u(\cdot)$ is the modified Bessel function of the first kind of order u , and $\mathcal{Q}_\mu(\dots)$ represents the generalized Marcum Q-function.

The κ - μ PDF/CDF in Eqs. (9–10) enables analysis of channels ranging from purely scattered ($\kappa = 0$) to strong line-of-sight ($\kappa \gg 1$). This flexibility is key for real deployment scenarios.

III. OUTAGE PROBABILITY ANALYSIS

This section explores the Outage Performance (OP) of receivers D_1 and D_2 of the considered system for symbols x_1 and x_2 over κ - μ fading channels. The OP can be defined as the probability that the instantaneous received SNR γ is less than a target threshold SNR, η_{th} . In Eqs. (13–18), we outline the derivations in detail for clarity. Each integral is solved using Marcum-Q expansions and series expansions, with references to [28]. Mathematically, the OP can be given as

$$\mathcal{P}_{out}(\eta_{th}) = \text{Prob}(\gamma < \eta_{th}) \quad (11)$$

A. Outage Probability for x_1

A symbol is said to be in an outage if its arrival at the receiver D_i for $i \in \{1, 2\}$ is unsuccessful. The symbol x_1 will go into outage if any of the communication links for x_1 to D_i ($S \rightarrow D_i$ or $S \rightarrow R \rightarrow D_i$) faces an outage.

The OP of x_1 at D_i over the indirect link $S \rightarrow R \rightarrow D_i$ can be expressed as:

$$\begin{aligned} \mathcal{P}_{out, e2e, x_1}(\eta_{th}) &= \text{Prob}(\min(\gamma_{SR, x_1}, \gamma_{SRD_i, x_1}) < \eta_{th}) \\ &= \mathcal{P}_{out, \gamma_{SR, x_1}}(\eta_{th}) + \mathcal{P}_{out, \gamma_{SRD_i, x_1}}(\eta_{th}) \\ &\quad - \mathcal{P}_{out, \gamma_{SR, x_1}}(\eta_{th}) \mathcal{P}_{out, \gamma_{SRD_i, x_1}}(\eta_{th}), \end{aligned} \quad (12)$$

where $\mathcal{P}_{out, \gamma_{SR, x_1}}(\eta_{th})$ and $\mathcal{P}_{out, \gamma_{SRD_i, x_1}}(\eta_{th})$ are the outage probabilities of x_1 over the links $S \rightarrow R$ and $R \rightarrow D_i$, respectively. $\mathcal{P}_{out, \gamma_{SR, x_1}}(\eta_{th})$ can be obtained as:

$$\begin{aligned} \mathcal{P}_{out, \gamma_{SR, x_1}}(\eta_{th}) &= \text{Prob}(\gamma_{SR, x_1} < \eta_{th}) \\ &= 1 - \mathcal{Q}_\mu \left(\sqrt{2\mu\kappa_{SR}}, \sqrt{\frac{2\mu(1+\kappa_{SR})\eta_{th}}{\rho\Psi_{SR}}} \right) \end{aligned} \quad (13)$$

The outage probability $\mathcal{P}_{out, \gamma_{SRD_i, x_1}}(\eta_{th})$ can be evaluated as:

$$\begin{aligned} \mathcal{P}_{out, \gamma_{SRD_i, x_1}}(\eta_{th}) &= \text{Prob}(\gamma_{SRD_i, x_1} < \eta_{th}) \\ &= \text{Prob} \left(\frac{\gamma_{RD_i}}{\gamma_{SD_i} + 1} < \eta_{th} \right) = \text{Prob}(\gamma_{RD_i} < \eta_{th}(\gamma_{SD_i} + 1)) \\ &= \int_0^\infty F_{\gamma_{RD_i}}(\eta_{th}(x+1)) f_{\gamma_{SD_i}}(x) dx \end{aligned} \quad (14)$$

By invoking the PDF and CDF of the instantaneous SNR from Eqs. (9–10) into Eq. (14), we can obtain the expression as:

$$\begin{aligned} \mathcal{P}_{out, \gamma_{SRD_i, x_1}}(\eta_{th}) &= 1 - \int_0^\infty \mathcal{Q}_\mu \left(\sqrt{2\mu\kappa_{RD_i}}, \sqrt{\frac{2\mu(1+\kappa_{RD_i})\eta_{th}(1+x)}{\rho\Psi_{RD_i}}} \right) \\ &\quad \times \frac{\mu}{\kappa_{SD_i}^{\frac{\mu-1}{2}} e^{\mu\kappa_{SD_i}}} \left(\frac{1+\kappa_{SD_i}}{\rho\Psi_{SD_i}} \right)^{\frac{\mu+1}{2}} x^{\frac{\mu-1}{2}} e^{-\frac{\mu(1+\kappa_{SD_i})x}{\rho\Psi_{SD_i}}} \times \\ &\quad I_{\mu-1} \left(2\mu \sqrt{\frac{\kappa_{SD_i}(1+\kappa_{SD_i})x}{\rho\Psi_{SD_i}}} \right) dx \end{aligned} \quad (15)$$

The Marcum-Q function in Eq. (15) can be replaced with its infinite series expansion as:

$$\mathcal{Q}_\mu(s, t) = \sum_{l=0}^\infty \sum_{k=0}^{\mu+l-1} \frac{s^{2l} t^{2k}}{l!k!2^{l+k}} e^{-\frac{s^2+t^2}{2}} \quad (16)$$

and therefore Eq. (15) can be simplified as:

$$\begin{aligned} \mathcal{P}_{out, \gamma_{SRD_i, x_1}}(\eta_{th}) &= 1 - \frac{\mu}{\kappa_{SD_i}^{\frac{\mu-1}{2}}} \left(\frac{1+\kappa_{SD_i}}{\rho\Psi_{SD_i}} \right)^{\frac{\mu+1}{2}} \\ &\quad \times e^{-\mu \left(\kappa_{SD_i} + \kappa_{RD_i} + \frac{(1+\kappa_{RD_i})\eta_{th}}{\rho\Psi_{RD_i}} \right)} \sum_{l=0}^\infty \sum_{k=0}^{\mu+l-1} \int_0^\infty (1+x)^k x^{\frac{\mu-1}{2}} \end{aligned}$$

$$\begin{aligned} & \times e^{-\frac{\mu}{\rho} \left(\frac{(1+\kappa_{RD_i})\eta_{th}}{\Psi_{RD_i}} + \frac{(1+\kappa_{SD_i})}{\Psi_{SD_i}} \right) x} \\ & \times I_{\mu-1} \left(2\mu \sqrt{\frac{\kappa_{SD_i}(1+\kappa_{SD_i})x}{\rho\Psi_{SD_i}}} \right) dx. \end{aligned} \quad (17)$$

Further, by using power series and with the help of [28, (3.15.2.5)], we obtain the expression as:

$$\begin{aligned} \mathcal{P}_{out, \gamma_{SRD_i, x_1}}(\eta_{th}) &= 1 - \frac{\mu}{\kappa_{SD_i}} \frac{\mu-1}{2} \left(\frac{1+\kappa_{SD_i}}{\rho\Psi_{SD_i}} \right)^{\frac{\mu+1}{2}} \\ & \times e^{-\mu \left(\frac{\kappa_{SD_i} + \kappa_{RD_i}}{\rho\Psi_{RD_i}} + \frac{(1+\kappa_{RD_i})\eta_{th}}{\rho\Psi_{RD_i}} \right)} \sum_{l=0}^{\infty} \sum_{k=0}^{\mu+l-1} \sum_{i=0}^k \frac{(\mu\kappa_{RD_i})^l}{l! k!} \\ & \times \binom{k}{i} \left(\frac{\mu(1+\kappa_{RD_i})\eta_{th}}{\rho\Psi_{RD_i}} \right)^k \left(\mu \sqrt{\frac{\kappa_{SD_i}(1+\kappa_{SD_i})}{\rho\Psi_{SD_i}}} \right)^{\mu-1} \\ & \times \frac{\Gamma(\mu+i)}{\Gamma(\mu)} \left(\frac{\rho}{\mu \left(\frac{(1+\kappa_{RD_i})\eta_{th}}{\Psi_{RD_i}} + \frac{1+\kappa_{SD_i}}{\Psi_{SD_i}} \right)} \right)^{\mu+i} \\ & \times {}_1F_1 \left(\mu+i; \mu; \frac{\mu \frac{\kappa_{SD_i}(1+\kappa_{SD_i})}{\Psi_{SD_i}}}{\frac{(1+\kappa_{RD_i})\eta_{th}}{\Psi_{RD_i}} + \frac{(1+\kappa_{SD_i})\eta_{th}}{\Psi_{SD_i}}} \right) \end{aligned} \quad (18)$$

By placing Eq. (13) and Eq. (18) into Eq. (12), we obtain the outage probability of x_1 for D_i over an indirect link via R .

The outage probability of x_1 at D_i for the direct link can be obtained as:

$$\begin{aligned} \mathcal{P}_{out, \gamma_{SD_i, x_1}}(\eta_{th}) &= \text{Prob}(\gamma_{SD_i, x_1} < \eta_{th}) \\ &= 1 - Q_{\mu} \left(\sqrt{2\mu\kappa_{SD_i}} \sqrt{\frac{2\mu(\kappa_{SD_i}+1)\eta_{th}}{\rho\Psi_{SD_i}}} \right) \end{aligned} \quad (19)$$

Finally, by considering that the selection combining technique is applied at the receiver, the expression of the total outage probability of x_1 at the receiver D_i can be evaluated as:

$$\mathcal{P}_{out, D_i, x_1}(\eta_{th}) = \mathcal{P}_{out, \gamma_{SD_i, x_1}}(\eta_{th}) \mathcal{P}_{out, e2e, x_1}(\eta_{th}). \quad (20)$$

B. Outage Probability for x_2

The symbol x_2 goes into outage if it cannot be decoded at the receivers D_1 and D_2 through the direct link.

1) Outage probability for x_2 with perfect SIC

By following the perfect SIC protocol, the symbol x_1 will initially be decoded, and further, it will be removed from the received signal. After the removal of x_1 , D_i detects x_2 . Therefore, if x_1 experiences an outage, x_2 cannot be detected at D_i . The outage probability of x_2 at D_i can be evaluated as

$$\begin{aligned} \mathcal{P}_{out, D_i, x_2}(\eta_{th}) &= \text{Prob}(\min(\gamma_{SD_i, x_2}, \gamma_{SRD_i, x_1}) < \eta_{th}) \\ &= \mathcal{P}_{out, \gamma_{SD_i, x_2}}(\eta_{th}) + \mathcal{P}_{out, \gamma_{SRD_i, x_1}}(\eta_{th}) \\ &\quad - \mathcal{P}_{out, \gamma_{SD_i, x_2}}(\eta_{th}) \mathcal{P}_{out, \gamma_{SRD_i, x_1}}(\eta_{th}) \end{aligned} \quad (21)$$

where $\mathcal{P}_{out, \gamma_{SD_i, x_2}}(\eta_{th})$ can be obtained using Eq. (10) as:

$$\begin{aligned} \mathcal{P}_{out, \gamma_{SD_i, x_2}}(\eta_{th}) &= \text{Prob}(\gamma_{SD_i, x_2} < \eta_{th}) \\ &= 1 - Q_{\mu} \left(\sqrt{2\mu\kappa_{SD_i}} \sqrt{\frac{2\mu(\kappa_{SD_i}+1)\eta_{th}}{\rho\Psi_{SD_i}}} \right) \end{aligned} \quad (22)$$

By placing Eq. (18) and Eqs. (22–21), the OP of x_2 for D_i is obtained.

2) Outage probability for x_2 with imperfect SIC

The outage probability of x_2 at the receivers in the considered

CRS-NOMA with imperfect SIC can be expressed as:

$$\begin{aligned} \mathcal{P}_{out, D_i, x_2}^{JP}(\eta_{th}) &= \text{Prob}(\min(\gamma_{SD_i, x_2}^{JP}, \gamma_{SRD_i, x_1}) < \eta_{th}) \\ &= \mathcal{P}_{out, \gamma_{SD_i, x_2}^{JP}}(\eta_{th}) + \mathcal{P}_{out, \gamma_{SRD_i, x_1}}(\eta_{th}) \\ &\quad - \mathcal{P}_{out, \gamma_{SD_i, x_2}^{JP}}(\eta_{th}) \mathcal{P}_{out, \gamma_{SRD_i, x_1}}(\eta_{th}) \end{aligned} \quad (23)$$

where $\mathcal{P}_{out, \gamma_{SD_i, x_2}^{JP}}(\eta_{th})$ can be evaluated as:

$$\begin{aligned} \mathcal{P}_{out, \gamma_{SD_i, x_2}^{JP}}(\eta_{th}) &= \text{Prob}(\gamma_{SD_i, x_2}^{JP} < \eta_{th}) \\ &= \text{Prob} \left(\frac{\rho |h_{SD_i}|^2}{\beta \rho |h_{RD_i}|^2 + 1} < \eta_{th} \right) \\ &= \int_0^{\infty} F_{\gamma_{SD_i}}(\eta_{th}(\beta x + 1)) f_{\gamma_{RD_i}}(x) dx. \end{aligned} \quad (24)$$

By invoking the CDF and PDF of γ_{SD_i} and γ_{RD_i} , respectively, we can rewrite the above equation as:

$$\begin{aligned} & \mathcal{P}_{out, \gamma_{SD_i, x_2}^{JP}}(\eta_{th}) \\ &= 1 - \int_0^{\infty} Q_{\mu} \left(\sqrt{2\mu\kappa_{SD_i}} \sqrt{\frac{2\mu(1+\kappa_{SD_i})\eta_{th}(1+\beta x)}{\rho\Psi_{SD_i}}} \right) \\ & \times \frac{\mu}{\kappa_{RD_i}^{\frac{\mu-1}{2}} e^{\mu\kappa_{RD_i}}} \left(\frac{1+\kappa_{RD_i}}{\rho\Psi_{RD_i}} \right)^{\frac{\mu+1}{2}} x^{\frac{\mu-1}{2}} e^{-\frac{\mu(1+\kappa_{RD_i})}{\rho\Psi_{RD_i}} x} \\ & \times I_{\mu-1} \left(2\mu \sqrt{\frac{\kappa_{RD_i}(1+\kappa_{RD_i})x}{\rho\Psi_{RD_i}}} \right) dx. \end{aligned} \quad (25)$$

Further, by expanding the Marcum-Q function and using power series, we can obtain the expression of outage probability of direct link $S \rightarrow D_i$ for x_2 as:

$$\mathcal{P}_{out, \gamma_{SD_i, x_2}^{JP}}(\eta_{th}) = 1 - \frac{\mu}{\kappa_{RD_i}^{\frac{\mu-1}{2}}} \left(\frac{1+\kappa_{RD_i}}{\rho\Psi_{RD_i}} \right)^{\frac{\mu+1}{2}}$$

$$\begin{aligned}
 & \times e^{-\mu \left(\kappa_{SD_i} + \kappa_{RD_i} + \frac{(1+\kappa_{SD_i})\eta_{th}}{\rho \Psi_{SD_i}} \right)} \sum_{l=0}^{\infty} \sum_{k=0}^{\mu+l-1} \sum_{i=0}^k \frac{(\mu \kappa_{SD_i})^l}{l! k!} \\
 & \times \binom{k}{i} \beta^i \left(\frac{\mu(1+\kappa_{SD_i})\eta_{th}}{\rho \Psi_{SD_i}} \right)^k \left(\mu \sqrt{\frac{\kappa_{RD_i}(1+\kappa_{RD_i})}{\rho \Psi_{RD_i}}} \right)^{\mu-i} \\
 & \times \frac{\Gamma(\mu+i)}{\Gamma(\mu)} \left(\frac{\rho \Psi_{SD_i} \Psi_{RD_i}}{\mu \left((1+\kappa_{RD_i}) \Psi_{SD_i} - (1+\kappa_{SD_i}) \beta \eta_{th} \Psi_{RD_i} \right)} \right)^{\mu+i} \\
 & \times {}_1F_1 \left(\mu+i; \mu; \frac{\mu \kappa_{RD_i} (1+\kappa_{RD_i}) \Psi_{SD_i}}{\left((1+\kappa_{RD_i}) \Psi_{SD_i} - (1+\kappa_{SD_i}) \beta \eta_{th} \Psi_{RD_i} \right)} \right). \quad (26)
 \end{aligned}$$

By placing Eq. (18) and Eq. (26) in Eq. (23), we get the outage probability of x_2 for the CRS-NOMA with imperfect SIC.

IV. ACHIEVABLE RATE ANALYSIS

In this section, we obtain the average achievable rates (ECs) of D_i , for $i \in \{1,2\}$ for symbols x_1 and x_2 . We can evaluate the average achievable rate by taking the average of the instantaneous achievable rate.

A. Achievable Rate for x_1

Since the source transmits the symbols in two time slots, the total instantaneous achievable rate of D_i for symbol x_1 can be given as [24, 26]:

$$\begin{aligned}
 \mathcal{R}_{D_i, x_1} &= \frac{1}{2} \min\{\log_2(1 + \gamma_{RD_i, x_1}), \log_2(1 + \gamma_{SR, x_1})\} \\
 &+ \frac{1}{2} \log_2(1 + \gamma_{SD_i, x_1}) \\
 &= \frac{1}{2} \log_2(1 + \gamma_{D_i, x_1}) + \frac{1}{2} \log_2(1 + \gamma_{SD_i, x_1}), \quad (27)
 \end{aligned}$$

where $\gamma_{D_i, x_1} = \min\{\gamma_{RD_i, x_1}, \gamma_{SR, x_1}\}$ [29]. The average achievable rate of D_i can be evaluated by taking the average of the instantaneous achievable rate as:

$$\bar{\mathcal{R}}_{D_i, x_1} = \frac{1}{2 \ln 2} \left\{ \int_0^{\infty} \ln(1+x) f_{\gamma_{D_i}}(x) dx + \int_0^{\infty} \ln(1+y) f_{\gamma_{SD_i, x_1}}(y) dy \right\} \quad (28)$$

The above expression can be written as [29]:

$$\bar{\mathcal{R}}_{D_i, x_1} = \frac{1}{2 \ln 2} \left\{ \underbrace{\int_0^{\infty} \frac{1-F_{\gamma_{D_i}}(x)}{1+x} dx}_{R_1} + \underbrace{\int_0^{\infty} \frac{1-F_{\gamma_{SD_i, x_1}}(y)}{1+y} dy}_{R_2} \right\} \quad (29)$$

where $F_{\gamma_{D_i}}(x)$ represents the CDF of $\gamma_{D_i, x_1} = \min\{\gamma_{RD_i, x_1}, \gamma_{SR, x_1}\}$, which can be obtained as:

$$\begin{aligned}
 F_{\gamma_{D_i}}(x) &= \mathcal{P}_{out, \gamma_{SR, x_1}}(x) + F_{\gamma_{RD_i, x_1}}(x) \\
 &- \mathcal{P}_{out, \gamma_{SR, x_1}}(x) F_{\gamma_{RD_i, x_1}}(x) \quad (30)
 \end{aligned}$$

where $F_{\gamma_{RD_i, x_1}}(x) = \text{Prob}(\gamma_{RD_i, x_2} < x) = 1 -$

$\mathcal{Q}_{\mu} \left(\sqrt{2\mu\kappa_{RD_i}}, \sqrt{\frac{2\mu(\kappa_{RD_i}+1)x}{\rho \Psi_{RD_i}}} \right)$. Further by invoking

$F_{\gamma_{RD_i, x_1}}(x)$ and $\mathcal{P}_{out, \gamma_{SR, x_1}}(x)$ from Eqs. (13–30) we get:

$$\begin{aligned}
 F_{\gamma_{D_i}}(x) &= 1 - \mathcal{Q}_{\mu} \left(\sqrt{2\mu\kappa_{RD_i}}, \sqrt{\frac{2\mu(\kappa_{RD_i}+1)x}{\rho \Psi_{RD_i}}} \right) \\
 &\times \mathcal{Q}_{\mu} \left(\sqrt{2\mu\kappa_{SR}}, \sqrt{\frac{2\mu(\kappa_{SR}+1)x}{\rho \Psi_{SR}}} \right). \quad (31)
 \end{aligned}$$

By invoking Eq. (31) into R_1 in Eq. (29), it can be expressed and further simplified with the help of Eq. (16) as:

$$\begin{aligned}
 R_1 &= \int_0^{\infty} \frac{1}{x+1} \mathcal{Q}_{\mu} \left(\sqrt{2\mu\kappa_{RD_i}}, \sqrt{\frac{2\mu(\kappa_{RD_i}+1)x}{\rho \Psi_{RD_i}}} \right) \\
 &\times \mathcal{Q}_{\mu} \left(\sqrt{2\mu\kappa_{SR}}, \sqrt{\frac{2\mu(\kappa_{SR}+1)x}{\rho \Psi_{SR}}} \right) dx \\
 &= e^{-\mu(\kappa_{RD_i} + \kappa_{SR})} \sum_{m=0}^{\infty} \sum_{n=0}^{\infty} \sum_{i=0}^{\mu+m-1} \sum_{j=0}^{\mu+n-1} \frac{\mu^{m+n+i+j}}{m! n! i! j!} \\
 &\times (\kappa_{RD_i})^m (\kappa_{SR})^n \left(\frac{1+\kappa_{RD_i}}{\rho \Psi_{RD_i}} \right)^i \left(\frac{1+\kappa_{SR}}{\rho \Psi_{SR}} \right)^j \\
 &\times \int_0^{\infty} \frac{x^{i+j}}{1+x} e^{-\frac{\mu}{\rho} \left(\frac{1+\kappa_{RD_i}}{\Psi_{RD_i}} + \frac{1+\kappa_{SR}}{\Psi_{SR}} \right) x} dx \quad (32)
 \end{aligned}$$

The integral in the above expression can be solved using [28, (2.1.3.6)], and finally, we get the expression as:

$$\begin{aligned}
 R_1 &= \sum_{m=0}^{\infty} \sum_{n=0}^{\infty} \sum_{i=0}^{\mu+m-1} \sum_{j=0}^{\mu+n-1} \frac{\mu^{m+n+i+j}}{m! n! i! j!} \Gamma(i+j+1) \\
 &\times \left(\frac{1+\kappa_{RD_i}}{\rho \Psi_{RD_i}} \right)^i \left(\frac{1+\kappa_{SR}}{\rho \Psi_{SR}} \right)^j (\kappa_{RD_i})^m (\kappa_{SR})^n \times \Gamma(-i-j, \\
 &\frac{\mu}{\rho} \left(\frac{1+\kappa_{RD_i}}{\Psi_{RD_i}} + \frac{1+\kappa_{SR}}{\Psi_{SR}} \right)) \times e^{-\frac{\mu}{\rho} \left(\frac{1+\kappa_{RD_i}}{\Psi_{RD_i}} + \frac{1+\kappa_{SR}}{\Psi_{SR}} \right) x} \quad (33)
 \end{aligned}$$

Further R_2 in Eq. (29) can be obtained as:

$$R_2 = \int_0^{\infty} \frac{1-F_{\gamma_{SD_i, x_1}}(y)}{1+y} dy = \int_0^{\infty} \frac{1}{1+y} \mathcal{Q}_{\mu} \left(\sqrt{2\mu\kappa_{SD_i}}, \sqrt{\frac{2\mu(1+\kappa_{SD_i})y}{\rho \Psi_{SD_i}}} \right) dy \quad (34)$$

Further, by using Eq. (16) and [28, (2.1.3.6)], we obtain the expression as:

$$\begin{aligned}
 R_2 &= \sum_{r=0}^{\infty} \sum_{j=0}^{\mu+r-1} \frac{\mu^{r+j}}{r! j!} \kappa_{SD_i}^r \left(\frac{1+\kappa_{SD_i}}{\rho \Psi_{SD_i}} \right)^j \Gamma(j+1) \\
 &\times \Gamma \left(-j, \frac{\mu(1+\kappa_{SD_i})}{\rho \Omega_{SD_i}} \right) e^{-\frac{\mu(1+\kappa_{SD_i})}{\rho} x} \quad (35)
 \end{aligned}$$

B. Achievable Rate for x_2

The instantaneous achievable rate of D_i for symbol x_2 can be given as:

$$\mathcal{R}_{D_i, x_2} = \frac{1}{2} \log_2(1 + \gamma_{SD_i, x_2}). \quad (36)$$

The average achievable rate of D_i for symbol x_2 can be evaluated using R_2 as:

$$\begin{aligned} \bar{\mathcal{R}}_{D_i, x_2} &= \frac{1}{2 \ln(2)} \int_0^\infty \frac{1 - F_{\gamma_{SD_i, x_2}}(y)}{1 + y} dy \\ &= \frac{1}{2 \ln(2)} \sum_{r=0}^\infty \sum_{j=0}^{\mu+r-1} \frac{\mu^{r+j}}{r! j!} \left(\frac{1 + \kappa_{SD_i}}{\rho \Psi_{SD_i}} \right)^j \Gamma(j + 1) \\ &\quad \times \Gamma\left(-j, \frac{\mu(1 + \kappa_{SD_i})}{\rho \Omega_{SD_i}}\right) \kappa_{SD_i}^r e^{\mu \left(\frac{1 + \kappa_{SD_i}}{\rho} - \kappa_{SD_i} \right)} \end{aligned} \quad (37)$$

The total average achievable rate of D_i is the sum of $\bar{\mathcal{R}}_{D_i, x_1}$ and $\bar{\mathcal{R}}_{D_i, x_2}$ as:

$$\bar{\mathcal{R}}_{D_i} = \bar{\mathcal{R}}_{D_i, x_1} + \bar{\mathcal{R}}_{D_i, x_2}. \quad (38)$$

Since the relay operates in a half-duplex, each symbol effectively occupies two-time slots, halving the nominal spectral efficiency. However, our scheme still exploits NOMA gains because the source transmits again in the second slot, improving overall throughput compared to conventional CRS, which remains silent after the first slot.

V. NUMERICAL AND SIMULATION RESULTS

In this section, we present the analytical results of the derived expressions and verify them through Monte Carlo simulations. In the CRS-NOMA system under consideration, we assume that the user D_1 is positioned significantly far from the source, resulting in a weak direct link between the source S and user D_1 . In contrast, the user D_2 is situated close to the source. Hence, the direct link between the source and user D_2 is stronger than the link between the source S and user D_1 . The parameters for the analytical results are given in the descriptions of their respective figures.

A. Simulation Setup and Parameter Table

We perform Monte Carlo simulations with 10^6 channel realizations, testing $\kappa \in \{0, 1, 2\}$, $\mu \in \{1, 2\}$, $\beta \in \{0, 0.01\}$, and Ψ_{ij} from 0–30 dB. Doubling the number of realizations yielded negligible changes (< 0.1 dB) in outage curves, indicating convergence. Table I summarizes these key parameters.

TABLE I. KEY SIMULATION PARAMETERS

Parameter	Value / Range
Number of realizations	10^6
κ	$\{0, 1, 2\}$
μ	$\{1, 2\}$
Residual interference β	$\{0, 0.01\}$
Path loss exponent	3
Ψ_{ij}	0–30 dB

Fig. 2 illustrates the outage probability versus transmit Signal-to-Noise Ratio (ρ) curves for various values of Ψ_{SD_1} .

The outage performance of both receivers for symbols x_1 and x_2 exhibits a significant improvement with increasing ρ , whereas the OP for symbol x_2 stabilizes in both users' medium and high SNR regimes. Additionally, the OP of D_1 for symbol x_2 decreases with Ψ_{SD_1} in the low SNR regime and increases with Ψ_{SD_1} in the high SNR region. In contrast, the outage performance of D_1 for symbol x_1 improves with Ψ_{SD_1} in the low and medium SNR ranges. Additionally, the outage probabilities of D_2 for both symbols x_1 and x_2 remain unaffected by Ψ_{SD_1} , as D_2 is not served through the $S \rightarrow D_1$ link. Moreover, we also showed the impact of residual interference due to the imperfect SIC applied to the receivers. It is clear from the curves that the OP of symbol x_2 degrades due to imperfect SIC.

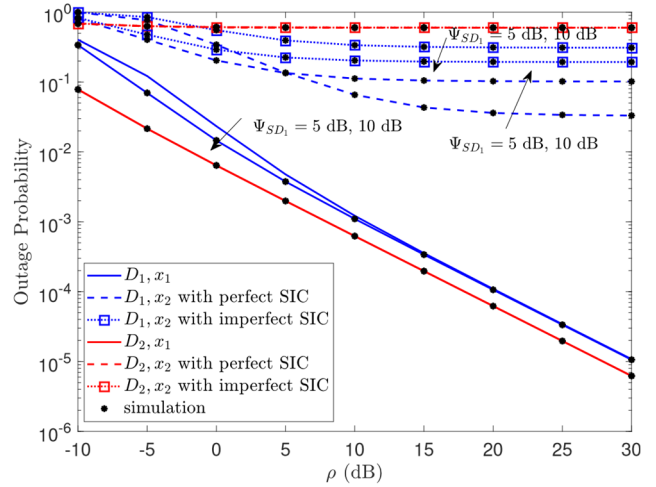


Fig. 2. Outage probability vs. ρ of the CRS-NOMA system over κ - μ fading channels with $\mu = 1$, $\beta = 0.01$, $\kappa_{SR} = \kappa_{RD1} = \kappa_{SD1} = \kappa_{SD2} = 1$, $\Psi_{SR} = 15$ dB, $\Psi_{RD1} = 20$ dB, $\Psi_{RD2} = 20$ dB, and $\Psi_{SD2} = 20$ dB.

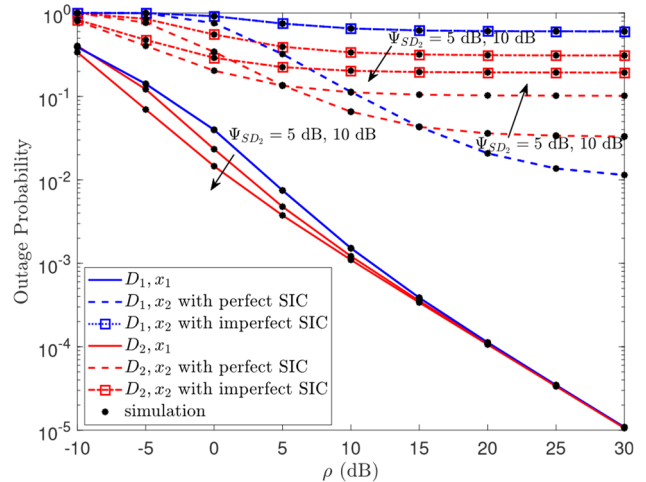


Fig. 3. Outage probability vs. ρ of the CRS-NOMA system over κ - μ fading channels with $\mu = 1$, $\beta = 0.01$, $\kappa_{SR} = \kappa_{RD1} = \kappa_{SD1} = \kappa_{SD2} = 1$, $\Psi_{SR} = 15$ dB, $\Psi_{RD1} = 20$ dB, $\Psi_{RD2} = 20$ dB, and $\Psi_{SD1} = 0$ dB.

Fig. 3 illustrates the curves depicting the relationship between OP and ρ for various values of Ψ_{SD_2} alongside fixed parameters as described. Notably, the OP of user D_1 remains constant irrespective of changes in Ψ_{SD_2} . Additionally, it is observed that the OP of D_2 for symbol x_1 exhibits improvement with increasing Ψ_{SD_2} in the low

and medium SNR regions. However, in the low SNR regime, the OP of D_2 improves, while it declines in the medium and high SNR regimes. The impact of imperfect SIC on OP of x_2 is also visible, indicating that the OP degrades with residual interference that occurs due to imperfect SIC.

Fig. 4 illustrates both system users' OP vs. ρ plots for different values of Ψ_{SR} for x_1 and x_2 . From the plots, it is clear that the OP of both users D_1 and D_2 for symbol x_1 improves with increasing Ψ_{SR} in the low and medium SNR regimes. However, the OP of both users for symbol x_2 remains unaffected by changes in Ψ_{SR} . These results can be justified because D_1 and D_2 receive only x_1 via the DF relay, whereas x_2 is transmitted directly from the source S to the users.

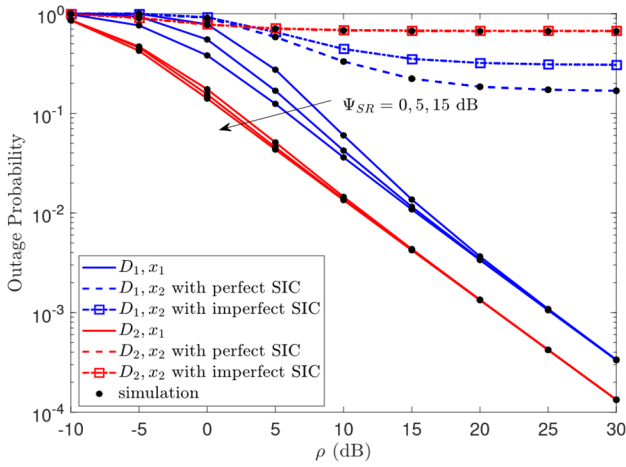


Fig. 4. Outage probability vs. SNR for different Ψ_{SR} with $\mu=1$, $\beta=0.01$, $\kappa_{SR}=\kappa_{RD1}=\kappa_{RD2}=\kappa_{SD1}=\kappa_{SD2}=0.01$, $\Psi_{RD1}=10$ dB, $\Psi_{RD2}=10$ dB, $\Psi_{SD1}=0$ dB, $\Psi_{SD2}=10$ dB.

Fig. 5 depicts the impact of residual interference levels on the OP of x_2 that occurred due to imperfect SIC to the receivers. We can observe from the curves that the OP performance remarkably reduces with β .

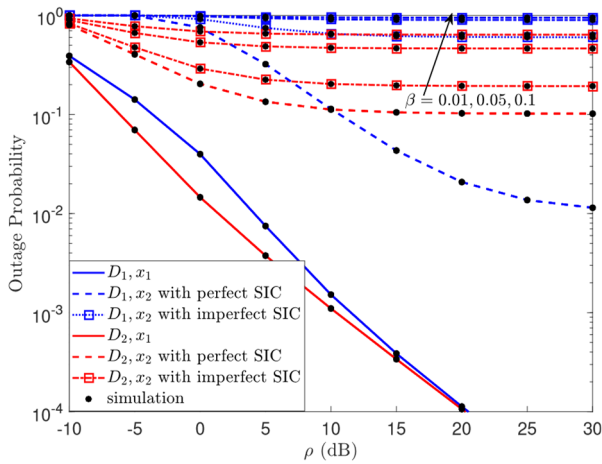


Fig. 5. Outage probability vs. SNR for different β with $\mu=1$, $\Psi_{SR}=15$ dB, $\kappa_{SR}=\kappa_{RD1}=\kappa_{RD2}=\kappa_{SD1}=\kappa_{SD2}=1$, $\Psi_{RD1}=10$ dB, $\Psi_{RD2}=20$ dB, $\Psi_{SD1}=0$ dB, $\Psi_{SD2}=10$ dB.

Fig. 6 illustrates the impact of the distance between the relay and the receivers on the outage performance of the considered system. For this analysis, we have taken the target threshold $\eta_{th}=2^{2R}-1$, where $R=0.2$ bits/second. The average channel gains of this system are modeled using the path-loss model as $\Psi_{ij}=(d_{ij}/d_0)^{-\nu}$ for $ij \in \{SR, SD_1, SD_2, RD_1, RD_2\}$, where $d_0=10$ m, $\nu=3$ is the path-loss exponent. From the curves, it is clear that the outage performance of both users improves when they come closer to the relay.

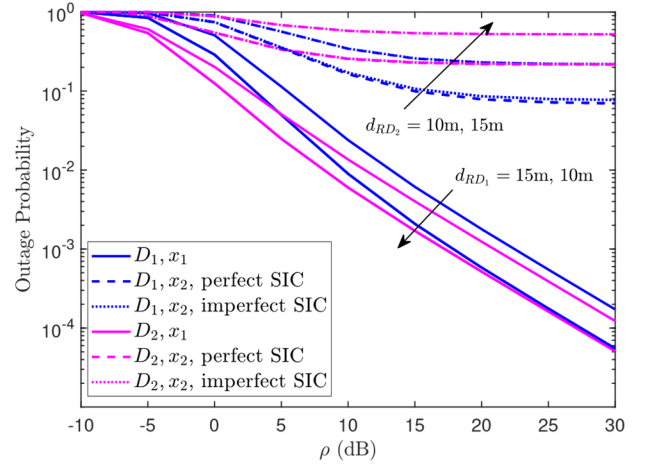


Fig. 6. Impact of distance on the outage probability vs. SNR for $\beta=0.01$ and target data rate $R=0.2$ bits/second with $\mu=1$, $d_{SR}=10$ m, $\kappa_{SR}=\kappa_{RD1}=\kappa_{RD2}=\kappa_{SD1}=\kappa_{SD2}=1$, $d_{SD1}=15$ m, $d_{SD2}=10$ m, $d_{SR}=10$ m.

The average achievable rates of all users and the system, considering symbols x_1 and x_2 , are presented in Figs. 7–Fig. 9, respectively, concerning the transmit SNR (ρ) for different κ - μ parameters and average received SNRs.

In Fig. 7, it is observed that the average achievable rates of individual users for both symbols increase with ρ . Notably, user D_2 outperforms D_1 in achievable rate due to its proximity to the source, resulting in a stronger channel link $S \rightarrow D_1$ compared to $S \rightarrow D_2$. Further, we can compare the achievable rates for the considered CRS-NOMA scheme and the conventional OMA scheme for D_1 and D_2 users. We can see that the CRS-NOMA scheme significantly outperforms the conventional OMA. This is due to the integration of the NOMA scheme with the cooperative relay system.

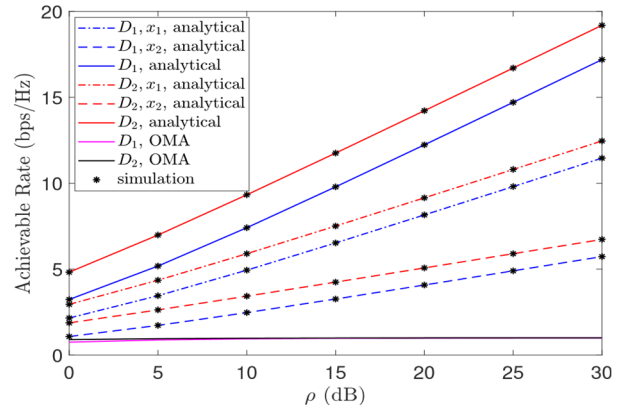


Fig. 7. Achievable rate vs. ρ with $\mu=1$, $\kappa_{SR}=\kappa_{RD1}=\kappa_{SD1}=\kappa_{SD2}=0.1$, $\Psi_{SR}=10$ dB, $\Psi_{RD1}=10$ dB, $\Psi_{RD2}=10$ dB, $\Psi_{SD1}=5$ dB and $\Psi_{SD2}=20$ dB.

Fig. 8 illustrates the average achievable rate performance against ρ for various values of μ , as described. The curves demonstrate that the average achievable rates increase with μ .

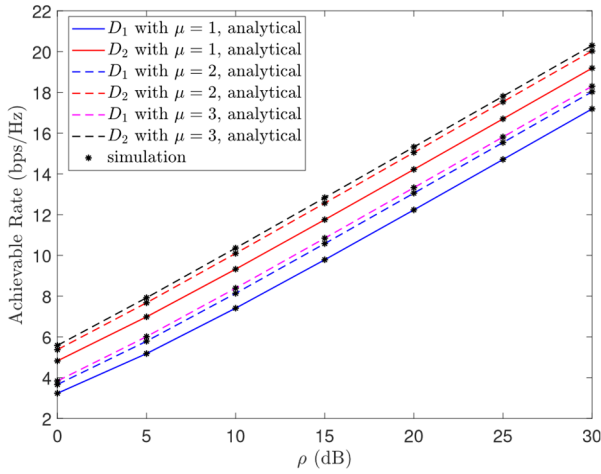


Fig. 8. Impact of fading on the achievable rate with the parameters, $\kappa_{SR} = \kappa_{RD1} = \kappa_{SD1} = \kappa_{SD2} = 0.1$, $\Psi_{SR} = 10$ dB, $\Psi_{RD1} = 10$ dB, $\Psi_{RD2} = 10$ dB, $\Psi_{SD1} = 5$ dB and $\Psi_{SD2} = 20$ dB.

Fig. 9 depicts the average achievable rate for different parameter κ values. It is evident that the average achievable rates of both users significantly improve for large values of κ .

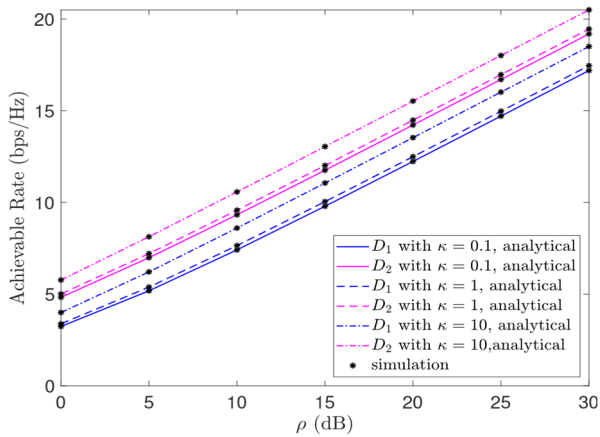


Fig. 9. Impact of κ on the achievable rate with the parameters $\mu = 1$, $\Psi_{SR} = 10$ dB, $\Psi_{RD1} = 10$ dB, $\Psi_{RD2} = 10$ dB, $\Psi_{SD1} = 5$ dB and $\Psi_{SD2} = 20$ dB.

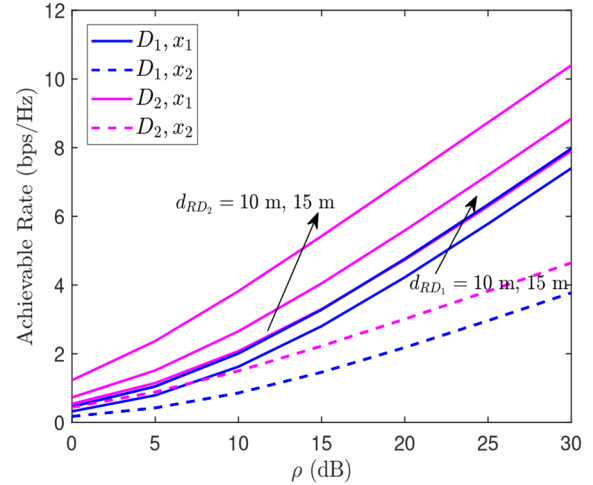


Fig. 10. Impact of distance on the achievable rate with the parameters, $\mu = 1$, $\kappa_{SR} = \kappa_{RD1} = \kappa_{SD1} = \kappa_{SD2} = 1$, $d_{SR} = 10$ m, $d_{SD1} = 10$ m, and $d_{SD2} = 10$ m.

In Fig. 10, we illustrate the impact of the distance between the relay and the receivers on the achievable rates of the users. From the curves, it is clear that the achievable rates of the users for only x_1 are affected by the distance between the relay and the users, whereas the attainable rates of users for the symbol x_2 are not affected by the distance between the relay and the users. Physically, as ρ increases, the outage decreases for both D_1 and D_2 . When $\beta > 0$, symbol x_2 suffers from imperfect SIC, hence a higher outage. This highlights the real-world implications of non-ideal cancellation.

VI. CONCLUSION

In this paper, we investigated the performance of the CRS-NOMA system in terms of Outage Probability (OP) and achievable rate over κ - μ fading channels. Specifically, we derived the closed-form expressions of the Cumulative Distribution Function (CDF) and Probability Density Function (PDF) for the instantaneous Signal-to-Noise Ratios (SNRs), from which the OP and the average achievable rate for both users, corresponding to symbols x_1 and x_2 , were obtained. We then examined the impact of channel parameters and average received SNRs on system performance. Since user D_2 is located closer to the source than D_1 , D_2 achieves better performance in terms of both OP and average achievable rate. We also compared the achievable rates of the proposed system with those of the conventional OMA scheme and investigated the effects of the relay–user distance on the outage probability and the average achievable rate. Finally, we validated these analytical findings through extensive Monte-Carlo simulations.

Unlike conventional CRS-NOMA models that require intricate power allocation, our proposed scheme transmits each symbol with maximum power. This choice simplifies system design, reduces computational overhead, and maintains robust performance, thereby making CRS-NOMA more amenable to real-world deployments. By avoiding complex power control mechanisms, our approach provides an efficient alternative to traditional

methods. In this paper, we do not account for mobility or network congestion, both of which can degrade performance in practical deployments. Additionally, our comparisons have centered on NOMA; future studies could investigate more advanced benchmarks or extend the system model to multi-relay networks.

CONFLICT OF INTEREST

The authors declare no conflict of interest.

AUTHOR CONTRIBUTIONS

Said Awad and Mohammed Abdel-Hafez: Conceptualization; Said Awad: Data curation; Said Awad and Mohammed Abdel-Hafez: Formal analysis, Funding acquisition, Investigation, Methodology; Said Awad: Simulation; Mohammed Abdel-Hafez: Supervision; Said Awad and Mohammed Abdel-Hafez: Writing – Original draft; Said Awad and Mohammed Abdel-Hafez: Writing – Review and editing; Both authors had approved the final version.

REFERENCES

- [1] L. Dai *et al.*, “Non-orthogonal multiple access for 5G: Solutions, challenges, opportunities, and future research trends,” *IEEE Communications Magazine*, vol. 53, no. 9, pp. 74–81, 2015.
- [2] Z. Ding *et al.*, “A survey on non-orthogonal multiple access for 5G networks: Research challenges and future trends,” *IEEE Journal on Selected Areas in Communications*, vol. 35, no. 10, pp. 2181–2195, 2017.
- [3] K. M. Rabie, B. Adebisi, E. H. Yousif, H. Gacanin, and A. M. Tonello, “A comparison between orthogonal and nonorthogonal multiple access in cooperative relaying power line communication systems,” *IEEE Access*, vol. 5, pp. 10118–10129, 2017.
- [4] D. T. Do and C. B. Le, “Application of NOMA in wireless system with wireless power transfer scheme: Outage and achievable rate performance analysis,” *Sensors*, vol. 18, no. 10, 2018.
- [5] N. Jaiswal and N. Purohit, “Performance analysis of NOMA enabled vehicular communication systems with transmit antenna selection over double Nakagami- m fading,” *IEEE Transactions on Vehicular Technology*, vol. 70, no. 12, pp. 12725–12741, 2021.
- [6] S. M. Awad and M. A. Hafez, “Achievable rate analysis of downlink NOMA systems over κ - μ shadowed fading channels,” in *Proc. 2023 IEEE Virtual Conference on Communications (VCC)*, NY, USA, pp. 241–245.
- [7] S. M. Awad and M. A. Hafez, “Outage performance analysis of downlink NOMA systems with imperfect SIC over κ - μ shadowed fading channels,” in *Proc. 2024 IEEE International Black Sea Conference on Communications and Networking (BlackSeaCom)*, Accepted, 2024.
- [8] A. Nosratinia, T. E. Hunter, and A. Hedayat, “Cooperative communication in wireless networks,” *IEEE Communications Magazine*, vol. 42, no. 10, pp. 74–80, 2004.
- [9] M. Zeng *et al.*, “Cooperative NOMA: State of the art, key techniques, and open challenges,” *IEEE Network*, vol. 34, no. 5, pp. 205–211, 2020.
- [10] M. Liaqat *et al.*, “Power-domain non-orthogonal multiple access (PD-NOMA) in cooperative networks: An overview,” *Wireless Networks*, vol. 26, pp. 181–203, 2020.
- [11] L. Lv, J. Chen, and Q. Ni, “Cooperative non-orthogonal multiple access in cognitive radio,” *IEEE Commun. Lett.*, vol. 20, no. 10, pp. 2059–2062, Oct. 2016.
- [12] S. Singh and M. Bansal, “Outage analysis of NOMA-based cooperative relay systems with imperfect SIC,” *Physical Communication*, vol. 43, 101219, 2020.
- [13] Y. Liu *et al.*, “Performance analysis of a downlink cooperative NOMA network over Nakagami- m fading channels,” *IEEE Access*, vol. 6, pp. 53034–53043, 2018.
- [14] N. G. Elakiya, K. Kandasamy, and M. D. Selvaraj, “Performance analysis of relay-based cooperative noma system,” *IEEE Wireless Antenna and Microwave Symposium (WAMS)*, pp. 1–5, 2022.
- [15] C. Wu *et al.*, “Achievable rate of NOMA-based DF relaying system with imperfect SIC over imperfect estimation of κ - μ shadowed fading channels,” *IEEE Communications Letters*, vol. 25, no. 7, pp. 2171–2175, 2021.
- [16] K. K. Godugu and S. Vappangi, “Investigations on secrecy performance of downlink overlay CR-NOMA system with SIC imperfections,” *IEEE Access*, 2024, pp. 18051–18072.
- [17] X. Yue *et al.*, “Performance analysis of NOMA with fixed gain relaying over Nakagami- m fading channels,” *IEEE Access*, vol. 5, pp. 5445–5454, 2017.
- [18] R. R. Kurup *et al.*, “Outage performance of cooperative noma system in lognormal fading channels,” in *Proc. IEEE International Conference on Electronics, Computing and Communication Technologies (CONECCT)*, 2020, pp. 1–6.
- [19] V. Kumar and M. F. Flanagan, “Performance analysis of NOMA-based cooperative relaying in alpha- μ fading channels,” *IEEE International Conference on Communications (ICC)*, pp. 1–7, 2019.
- [20] R. Jiao *et al.*, “On the performance of NOMA-based cooperative relaying systems over Rician fading channels,” *IEEE Transactions on Vehicular Technology*, vol. 66, no. 12, pp. 11409–11413, 2017.
- [21] Y. Li *et al.*, “Outage performance enhancement for NOMA-based cooperative relay sharing networks,” *IEEE Wireless Communications Letters*, vol. 11, no. 12, pp. 2665–2669, 2020.
- [22] H. Liu, Z. Ding, K. J. Kim, K. S. Kwak, and H. V. Poor, “Decode-and forward relaying for cooperative NOMA systems with direct links,” *IEEE Transactions on Wireless Communications*, vol. 17, no. 12, pp. 8077–8093, Dec. 2018.
- [23] G. Nagesham and S. Vappangi, “Performance of selective DF relay aided cooperative NOMA under imperfect SIC,” in *Proc. 2023 3rd International Conference on Mobile Networks and Wireless Communications (ICMNWC)*, 2023, pp. 1–8.
- [24] P. K. Jha and D. S. Kumar, “Achievable rate analysis of relay assisted cooperative NOMA over Rician fading channels,” in *Proc. 4th international conference on recent advances in information technology (RAIT)*, 2018, pp. 1–5.
- [25] S. Khatalin and M. Hadeel, “On the performance of cooperative relaying systems with NOMA in κ - μ fading environment,” *Wireless Communications and Mobile Computing*, 1319687, 2022.
- [26] J. Zhang *et al.*, “Performance analysis of relay assisted cooperative non-orthogonal multiple access systems,” *IEEE Wireless Commun. Letter*, pp. 1–5, 2017.
- [27] M. D. Yacoub, “The κ - μ distribution and the η - μ distribution,” *IEEE Antennas and Propagation Magazine*, vol. 49, no. 1, pp. 68–81, 2007.
- [28] A. P. Prudnikov, Y. A. Brychkov, and O. I. Marichev, *Integrals, and Series Special Functions*. New York, NY, USA: Gordon and Breach Science Publishers, 1986.
- [29] K. P. Peppas, “Dual-hop relaying communications with cochannel interference over η - μ fading channels,” *IEEE Transactions on Vehicular Technology*, vol. 62, no. 8, pp. 4110–4116, Oct. 2013.

Copyright © 2025 by the authors. This is an open access article distributed under the Creative Commons Attribution License which permits unrestricted use, distribution, and reproduction in any medium, provided the original work is properly cited ([CC BY 4.0](https://creativecommons.org/licenses/by/4.0/)).